Ultrastructure of the life-cycle stages of *Goussia janae* (Apicomplexa, Eimeriidae), with X-ray microanalysis of accompanying precipitates

JULIUS LUKEŠ[1]
Institute of Parasitology, Czech Academy of Sciences, Branišovská 31, 37005 České Budějovice, Czechoslovakia

AND

VLADIMÍR STARÝ
Institute of Microbiology, Czech Academy of Sciences, Vídeňská 1083, 14220 Prague, Czechoslovakia

Received March 4, 1992
Accepted June 19, 1992

LUKEŠ, J., and STARÝ, V. 1992. Ultrastructure of the life-cycle stages of *Goussia janae* (Apicomplexa, Eimeriidae), with X-ray microanalysis of accompanying precipitates. Can. J. Zool. **70**: 2382–2397.

The ultrastructural features of the life-cycle stages of *Goussia janae* from the intestinal epithelium of the dace *Leuciscus leuciscus* and chub *L. cephalus* are described. All merogonial, gamogonial, and early sporogonial stages were localized in the microvillar region in an intracellular and extracytoplasmic position, covered by closely apposed enterocyte and parasitophorous vacuole membranes. Two types of location in the host cell were observed: (*i*) a more frequent "monopodial" type with a single zone of attachment to the host-cell cytoplasm, and (*ii*) a "spider-like" type with several isolated zones of attachment. Merozoites were formed by either ecto- or endo-merogony. Microgamonts produced elongated biflagellate microgametes at their periphery. The oocyst wall, produced exclusively by the parasite, was formed at the end of the intracellular phase of the life cycle. Exogenous sporulation resulted in the formation of elongated sporocysts with a thin sporocyst wall bearing a longitudinal suture accompanied by a narrow membranaceous veil. In the cytoplasm and cytoplasmic and parasitophorous vacuoles of the parasite, fine, dense precipitates were present. X-ray microanalysis of these precipitates from osmicated and non-osmicated samples revealed high levels of Ca and P, indicating the possible presence of hydroxyapatite.

LUKEŠ, J., et STARÝ, V. 1992. Ultrastructure of the life-cycle stages of *Goussia janae* (Apicomplexa, Eimeriidae), with X-ray microanalysis of accompanying precipitates. Can. J. Zool. **70** : 2382–2397.

On trouvera ici la description des caractéristiques ultrastructurales des différents stades de *Goussia janae* dans l'épithélium intestinal des mulets *Leuciscus leuciscus* et *L. cephalus*. Tous les stades, mérogonie, gamogonie et sporogonie en début de formation, ont été trouvés dans la région microvillaire en position intracellulaire et extracytoplasmique, entourés d'une couche serrée de membranes vacuolaires entérocytiques et parasitophores. Deux types d'attachement à l'intérieur de la cellule hôte ont été observés : (*i*) un type « monopode », comportant une seule zone d'attachement au cytoplasme de l'hôte, et (*ii*) un type « arachnoïde », comportant plusieurs zones isolées d'attachement. Les mérozoïtes se forment par ectomérogonie ou par endomérogonie. Les microgamontes produisent à leur périphérie des microgamètes allongées, à deux flagelles. La paroi de l'oocyste, synthétisée entièrement par le parasite, se forme à la fin de la phase intracellulaire du cycle. La sporulation exogène aboutit à la formation de sporocystes allongés, à paroi mince, portant une suture longitudinale ornée d'un voile étroit et membraneux. Dans le cytoplasme, on observe les vacuoles cytoplasmiques et les vacuoles parasitophores du parasite, de même que des précipités compacts et opaques. La micro-analyse aux rayons X de ces précipités prélevés dans des échantillons traités à l'acide osmique et dans des échantillons non traités a révélé la présence de concentrations élevées de Ca et de P, ce qui indique peut-être la présence d'hydroxyapatite.

[Traduit par la rédaction]

Introduction

The intestine of several marine and freshwater fish is parasitized not only by intracytoplasmic coccidia but also by many species with developmental stages localized in the microvillar region of enterocytes (Molnár 1989). At the ultrastructural level, these coccidia differ from *Cryptosporidia*, which inhabit the same region of the gut of higher vertebrates (Current and Reese 1986), especially by the presence of flagellated microgametes and the absence of a feeding organelle, and in the structure of the oocyst and sporocyst walls (Morrison and Poynton 1989; Jastrzebski and Komorowski 1990; Lukeš 1992*a*).

We describe herein the ultrastructure of the life-cycle stages of *Goussia janae* from the gut of a dace and a chub. The results of light microscopical and pathogenicity studies of this extracytoplasmic coccidium were published previously (Lukeš and Dyková 1990).

During the examination of our material in the electron microscope, we frequently found dense precipitates, the occurrence of which was not incidental. We therefore concluded that we should perform a semiquantitative analysis of these precipitates using the X-ray microanalysis method.

Materials and methods

Transmission electron microscopy (TEM)

The dace *Leuciscus leuciscus* and chub *L. cephalus* used in this study were caught in the Černovický Potok Brook, Soběslav, and the Malše river, Římov, both in southern Bohemia. Small parts of the anterior, central, and posterior parts of the infected intestine of 10 daces and 4 chubs were fixed in 4% OsO_4 in 0.2 M cacodylate buffer, pH 7.2, for 1 h at 4°C, then dehydrated in graded series of ethanol and embedded in Epon–Araldite resin. Thin sections were cut with glass knives on an LKB Ultrotome III, stained with uranyl acetate and lead citrate (Venable and Coggeshall 1965), and examined in a Philips 420 electron microscope.

To study exogenous sporulation, the faeces and faecal casts were incubated in tap water at 10°C for 24–48 h. The faecal casts containing the sporulation stages were homogenized with a Potter–Elvehjem homogenizer and fixed and processed as described above. Thin sections with oocysts were placed on Formvar-coated grids. Since the dense precipitates were detected in the thin sections, the following

[1]Author to whom all correspondence should be addressed.

Printed in Canada / Imprimé au Canada

fixation and staining procedures were used with later samples: (*i*) fixation in 3% glutaraldehyde in 0.2 M cacodylate buffer overnight, followed by dehydration and embedding in Epon–Araldite (Roth and Heitz 1989); (*ii*) fixation in 4% paraformaldehyde and embedding in LR White resin (Roth and Heitz 1989); (*iii*) staining of thin sections with modified Sato's lead stain for 2–3 min (Hanaichi et al. 1986); (*iv*) en bloc staining with a 2% solution of uranyl acetate for 15 min before gradual dehydration (Hayat 1975); (*v*) treating the sections with 0.5 N HCl or 1% ethylenediaminetetraacetic acid (EDTA) for 2 min before uranyl acetate and lead citrate staining (Mollenhauer 1987).

Scanning electron microscopy

Oocysts in polylysine on glass cover slips and small pieces of infected tissue were fixed in 2% OsO_4 in 0.2 M cacodylate buffer at 4°C for 1 h and washed in the same buffer at 4°C for 30 min. They were dehydrated, then infiltrated with increasing concentrations of acetate, critical-point dried in a Polaron E 3000, and sputter-coated with gold in a Polaron E 5100 coater. The specimens were examined using a Tesla BS 300 scanning electron microscope (SEM).

X-ray microanalysis

Thin sections (0.09–0.1 μm) were collected on either Cu or Ni grids (mesh 200), carbon coated, and observed in a Philips CM 12 electron microscope equipped with an EDAX 9900 analyzer. The X-radiation study was carried out with a Si (Li) detector (about 160 eV resolution) with thin Be window. Microanalysis was done in a Be low-background holder tilted 20° to the detector, using a beam of 30 nm diameter and an accelerating voltage of 120 kV, at a magnification of 30 000 ×. The spectra were collected in 200 s live time, a typical X-ray count rate being around 400–600 cps (1 cps = 1 Bq). The precipitates, parasite cytoplasm, dense-granule content, enterocyte cytoplasm, Epon–Araldite resin, and LR White resin (Kent and Kendall 1988) were analyzed.

Results

Location in the host cell

Zoites with their apical parts directed towards the enterocytes are shown in Figs. 1 and 2 shortly before invasion of the host cell. Except for these motile zoites, all merogonial, gamogonial, and early sporogonial stages were localized intracellularly in the enterocytes between the cell membrane and the cytoplasm in a location that can be termed extracytoplasmic (EC) (Figs. 3–36).

However, two groups of these stages could be distinguished with reference to their location in the host cell. The most frequent stages, designated "monopodial," were found in the microvillous region of the enterocytes (Figs. 4, 6, 8). On the luminal site (facing the gut lumen) they were covered by two host-cell-derived membranes, the outer of which was the enterocyte membrane and the inner one the parasitophorous vacuole (PV) membrane (Fig. 7). The two membranes were so closely apposed to each other that there was no cytoplasm between them and their total thickness was 20 nm (Fig. 7). In one large area in contact with the enterocyte cytoplasm (and therefore monopodial), the parasite was separated only by the PV membrane, which enclosed it within a narrow parasitophorous vacuole (Figs. 6, 8).

The second type of intracellular and EC stage is termed "spider-like" because its location in the intestine gives it the appearance of a spider (Figs. 12, 13, 18, 24, and 26). The stages of this type were also covered by the enterocyte and PV membranes (Fig. 7); however, in contrast to the above-mentioned monopodial stages, they were localized above the microvillous region of the enterocytes. They were connected with the host-cell cytoplasm only by two or more projections (Figs. 12, 13, 24). The initial phase of the formation of a spider-like meront is visible in Figs. 10 and 23, where the enterocyte and PV membranes enclosing a parasite exhibit small undulations which subsequently become prominent projections (Fig. 24). At the tips of these projections, multiple fusions of the enterocyte membrane covering the parasite with adjacent microvilli occurred (Figs. 10, 24), thus creating another connection between this stage and the enterocyte. During this fusion process, the fibrillar content of the microvilli was drawn in between the two membranes (Fig. 9). The enterocyte membrane retained (for a short time) a wavy shape reminiscent of that of the fused microvilli; this can be seen in the oblique section through the periphery of a meront (Fig. 9). Later, it again became closely apposed to the underlying PV membrane. The transverse section through a spider-like stage shows that the PV membrane penetrated the newly established connection until it made contact with the host-cell cytoplasm (Figs. 11, 12). Some spider-like stages were connected via the projections of the enterocyte and PV membranes with two (Fig. 13) or more (Fig. 26) enterocyte cytoplasms (see Discussion).

Merogonial stages

The earliest developmental stages observed in our material were small oval meronts (Figs. 4, 5). They were surrounded by a trilaminar pellicle and contained a large centrally located nucleus with a prominent nucleolus, mitochondria, micropore, lipid granules, Golgi apparatus, endoplasmic reticulum, and small electron-lucent vacuoles (Fig. 6). At the periphery of the meront, a persistent apical complex composed of a polar ring, a conoid, two preconoidal rings, and sparse electron-dense micronemes was present (Fig. 14). Scattered floccular material was visible in the PV contents of most merogonial stages (Figs. 8, 11, 12). In some parts of the infected intestine, especially the anterior region, these oval meronts blanketed almost the whole surface of the intestinal mucosa (Fig. 5).

The merozoites were apparently formed by both ecto- and endo-merogonial division; however, the former type of division was far more frequent in all samples studied. At the beginning of ectomerogony, the nucleus underwent multiple division, and invaginations of the meront cytoplasm (Fig. 15) subsequently led to the detachment of 4–10 merozoites, leaving a small part of the cytoplasm behind (Figs. 16, 17).

In rare instances some meronts, the cytoplasm of which contained several dense granules, gave rise to merozoites by endomerogony (Figs. 19–21). The precise number of merozoites that originated by this type of division is unknown, but there were at least five (Figs. 19–21). The number of merogonial divisions could not be established because only naturally infected fish were available. However, it is obvious that there are at least two merogonial generations in the life cycle of *G. janae*.

Gamogonial stages

Gamogonial development began with meronts that had similar morphological features to the meronts that gave rise to the merozoites. Immature macrogamonts could be distinguished by the presence of a large elongated nucleus with a prominent oval nucleolus (Fig. 22). They also contained small round electron-lucent amylopectin granules, large, less numerous lipid inclusions, a persistent peripherally located conoid formed by polar and preconoidal rings, and remnants of micronemes (Fig. 22). The growing, dense round granules with non-homogeneous contents and multiple concentric layers of

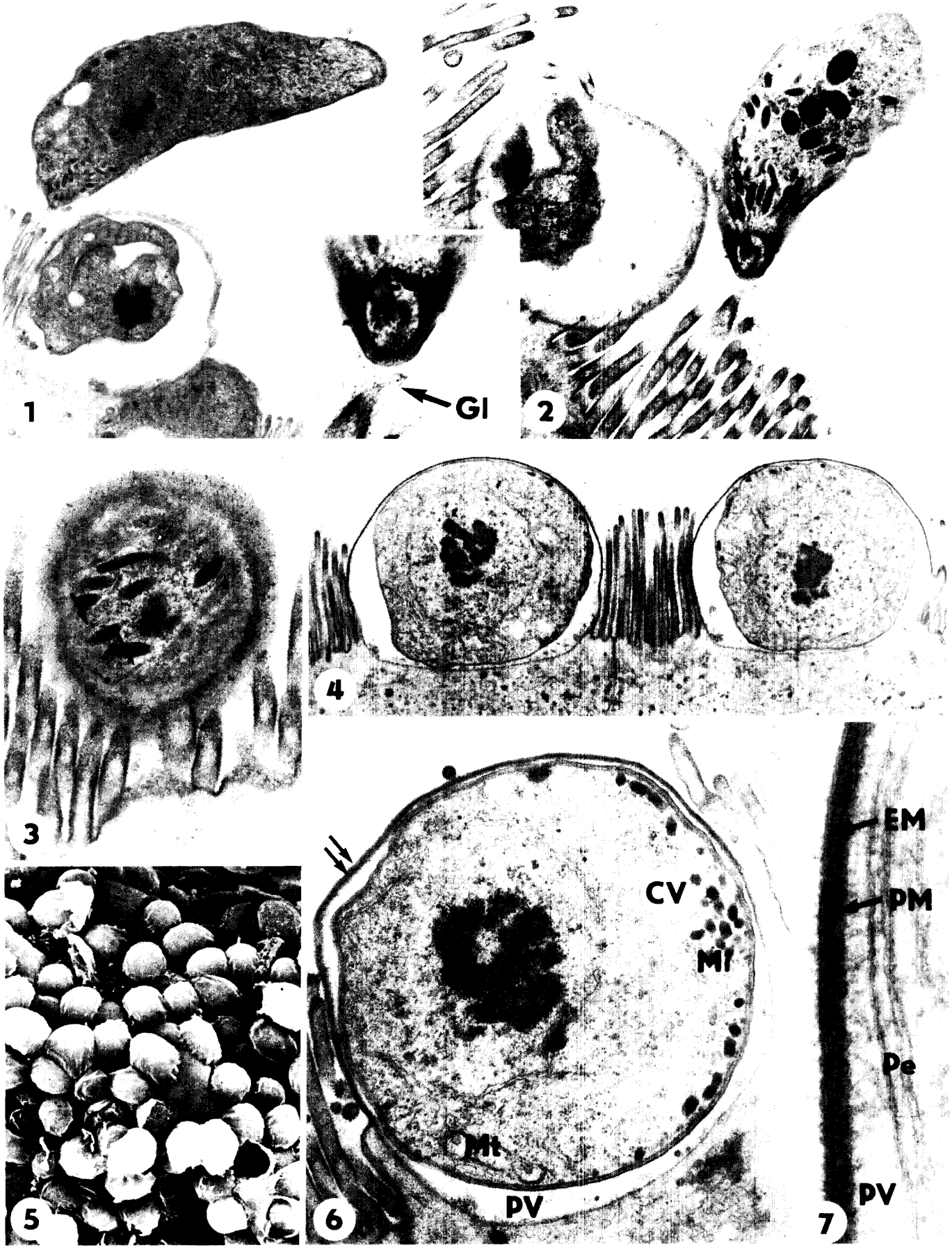

endoplasmic reticulum were typical of more advanced stages (Figs. 22, 23). Although the amylopectin granules grew steadily in number and dimensions, the lipid inclusions and dense granules remained almost the same throughout macrogametogenesis (Fig. 25).

Young microgamonts contained numerous nuclei with irregularly arranged heterochromatin, cisternae of granular endoplasmic reticulum, and small amylopectin granules (Fig. 27). The remnants of micronemes were also present in some immature microgamonts. The number of lipid inclusions remained low during microgametogenesis (Fig. 28). Further development led to the formation of deep invaginations on the surface of the microgamont, followed by the emergence of microgametes (Figs. 28 and 29). As microgamete formation proceeded, the perforatorium Anlage arose close to each nucleus and protruded into the parasitophorous vacuole (Fig. 29). An electron-dense portion of the nucleus gradually separated from the residual granular portion. The former became part of a newly formed microgamete, while the latter was left behind in the residual cytoplasm (Fig. 29). At this stage the parasitophorous vacuole became enlarged and contained fine, filamentous material (Fig. 30).

The mature microgametes exhibited prominent apical perforatorium with a slightly curved tip (Fig. 31), an elongated mitochondrium, a large homogeneous nucleus, and two flagella connected to basal bodies behind the perforatorium (Figs. 30, 31).

Sporogonial stages

Endogenous sporulation

Endogenous sporulation occurred largely in the EC location within the enterocyte (Figs. 32–36). After fertilization the cytoplasm of the large oval macrogamont became filled with amylopectin, lipid, and dense granules (Fig. 36). Numerous concentric layers of endoplasmic reticulum appeared beneath the limiting pellicle of the early sporont. They participated in the formation of the oocyst and sporocyst walls of the future sporulation stages. The young sporont was enclosed first by one envelope (Fig. 32) and later by two envelopes (Figs. 33–36). By the time they had become detached from the sporont cytoplasm into the parasitophorous vacuole, they had already lost the appearance of functional bilayered membranes and were homogeneously dense (Figs. 34, 35). While still in the EC location within the enterocyte they became closely apposed to each other and formed a bilayered oocyst wall (Fig. 36). At this stage the foundations of the sporocyst wall were subtended by a trimembraneous pellicle (Figs. 34, 35). During later development the two membranes (enterocyte and PV) derived from the host cell ruptured and the sporont was released in the gut lumen, where it became part of the casts that left the host with the other faeces (Fig. 37).

Exogenous sporulation

Development continued in water, multiple cleavage of the sporont cytoplasm resulting in the formation of four sporocysts containing two sporozoites each (Fig. 38). The immature sporozoites contained a large nucleus with scattered chromatin, numerous ribosomes, amylopectin granules, and a prominent crystalloid body in their cytoplasm (Fig. 38).

At this stage both the oocyst and sporocyst walls, which are quite similar in structure, were already formed (Fig. 39). The sporocyst wall consisted of an inner electron-dense layer covered with an outer 7-nm electron-lucent layer. The inner layer was of uniform thickness (about 18 nm) except where it gave rise to a small suture (about 65 nm thick) (Figs. 39–41). This longitudinal suture divided the sporocyst wall into two identical shelves (Fig. 42). Within the suture a thin interposing strip was inserted between the two shelves (Fig. 40). In some micrographs (Figs. 39 and 40) a very narrow (about 30 nm)

FIGS. 1–7. Transmission and scanning electron micrographs of early merogonial stages of *Goussia janae*. Fig. 1. Zoite prior to invasion of the host cell. The apical complex is outside the section. × 12 500. Fig. 2. Another invading zoite with its apical part approaching the microvilli. × 21 500. Inset: The conoid (Co) appears to be in close contact with the glycocalyx (Gl) on the tips of the microvilli. × 40 500. Fig. 3. Oblique section through an invading zoite within the microvillous region of the enterocyte. Several subpellicular microtubules (arrows) are visible. × 36 500. Fig. 4. Early meronts protruding slightly above the microvillous region of individual enterocytes. ×9800. Fig. 5. Anterior part of the intestine heavily infected with merogonial stages. ×2200. Fig. 6. Round early meront covered on its luminar part by two membranes: the enterocyte and parasitophorous vacuole membranes (double arrows). A large nucleus, prominent nucleolus, peripherally scattered micronemes (Mi), cytoplasmic vacuole (CV), ribosomes and mitochondrion (Mt) are visible in this section. × 28 900. Fig. 7. Periphery of an early meront. The trimembraneous pellicle (Pe) is covered by enterocyte (EM) and parasitophorous vacuole (PM) membranes. PV, parasitophorous vacuole contents. × 175 000.

FIGS. 8–15. Transmission electron micrographs of "monopodial" and "spider-like" meronts of *Goussia janae*. Fig. 8. A more advanced monopodial meront containing a large lipid inclusion (LI) and dense, floccular material (DM) scattered in its parasitophorous vacuole. The arrow indicates the remnants of a peripherally fused microvillus. × 15 000. Fig. 9. Transverse section through a growing monopodial meront with a continuous row of multiple fusions between the microvilli and the enterocyte membrane covering the parasite. Mv, microvilli; EM, enterocyte membrane; PM, parasitophorous vacuole membrane. × 36 500. Fig. 10. Clusters of fusions (asterisks) between individual microvilli and projections of the enterocyte membrane covering a spider-like meront. × 24 000. Fig. 11. Longitudinal section through an early spider-like attachment of a meront. The parasitophorous vacuole (PV) contains dense material (DM), probably the remnants of fused microvilli. × 17 000. Fig. 12. A spider-like meront, in this case with six regions of attachment to a single enterocyte. A dense precipitate is visible in the PV contents. × 17 200. Fig. 13. Another spider-like meront extracytoplasmic to two enterocytes (HC1 and HC2) via multiple projections (asterisks). × 13 400. Fig. 14. Apical complex of a round meront. The conoid (Co), polar ring (PR), micronemes (Mi), and trimembraneous pellicle (Pe) still persist. × 62 500. Fig. 15. Advanced meront with a large centrally located nucleus. The prominent cytoplasmic projection (CP) represents commencement of a merogonial division. × 17 300.

FIGS. 16–21. Transmission electron micrograph showing merogonial division in *Goussia janae*. Fig. 16. An early stage of ectomerogenial division, with numerous merozoites protruding from the residual cytoplasm (RC). × 10 500. Fig. 17. Meront containing several mature merozoites. Asterisks indicate small projections which eventually fuse with adjacent microvilli and thus form a new zone of attachment. × 10 500. Fig. 18. A spider-like meront with three mature merozoites visible. × 12 000. Fig. 19. An early stage of endomerogenial division. The nucleus has divided and small sections of newly formed pellicle are present (arrows), although a persistent conoid (Co) from the former meront still remains. Rh, rhoptries. × 12 700. Fig. 20. A more advanced meront, in the cytoplasm of which at least five merozoites are formed by endomerogeny. Mi, micronemes × 11 500. Fig. 21. Nearly mature merozoites in the cytoplasm of a large monopodial meront. × 12 500.

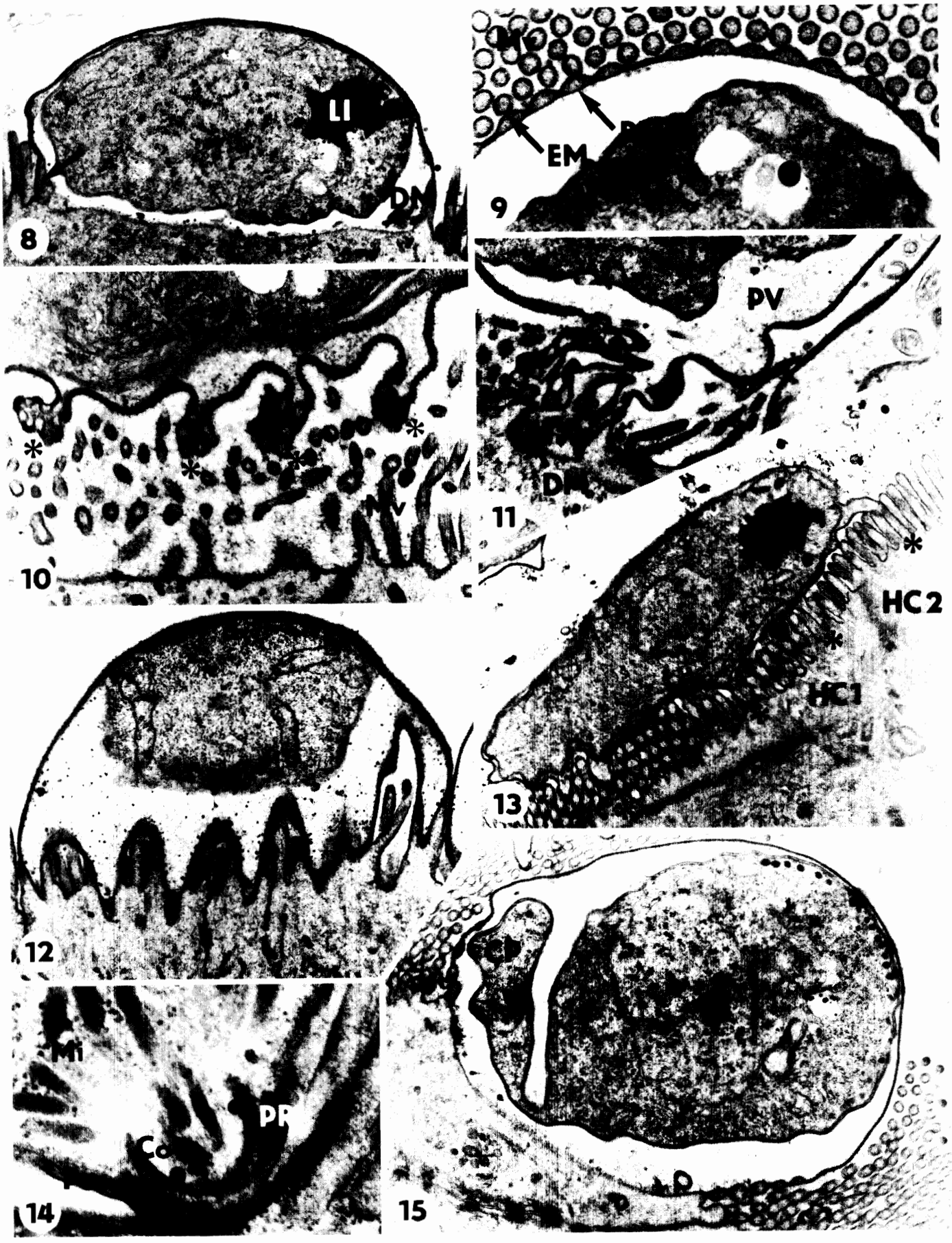

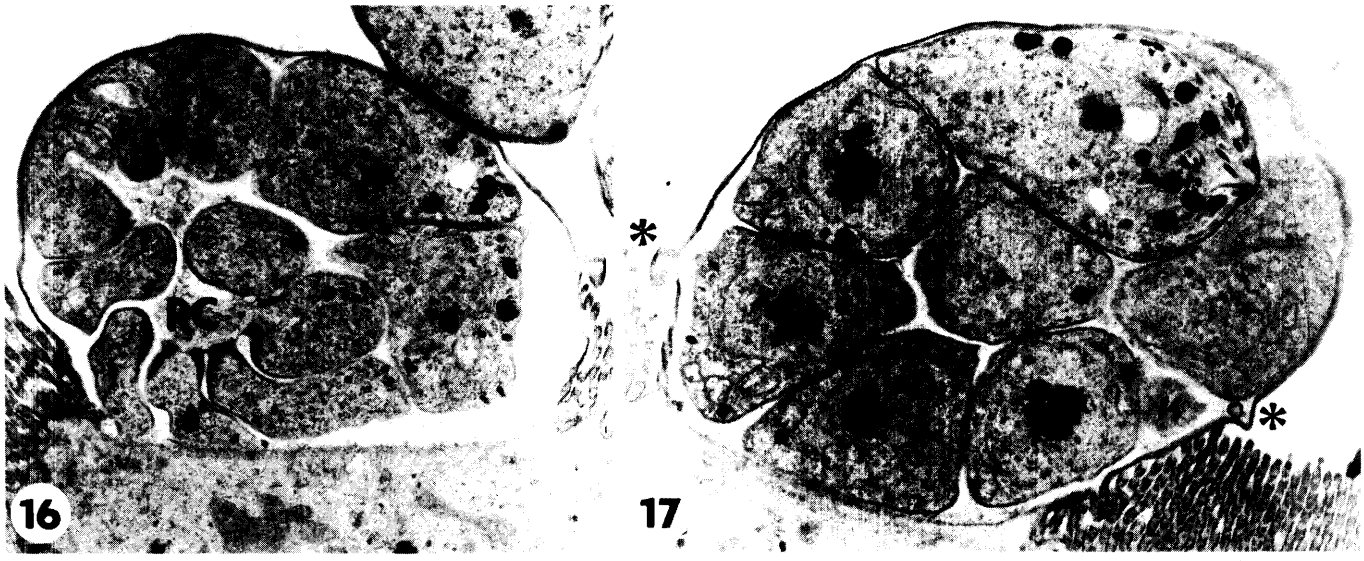

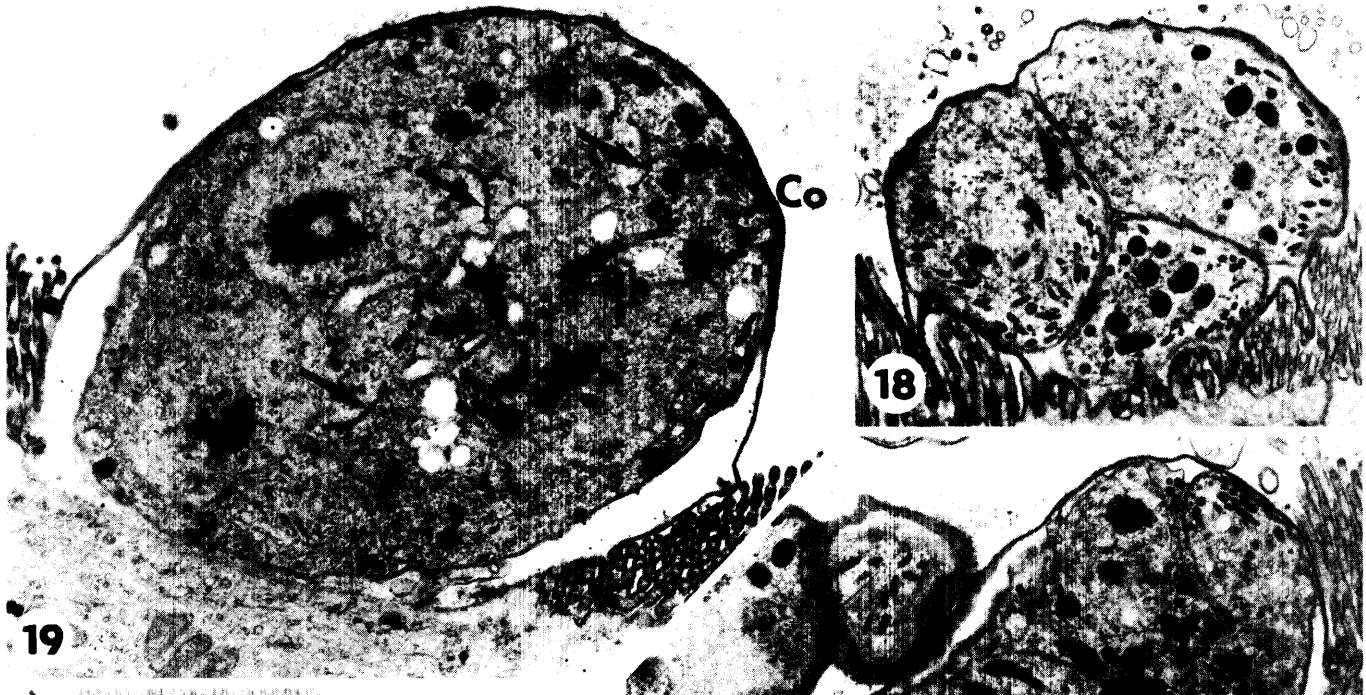

FIGS. 22–26. Transmission electron micrographs showing macrogametogenesis in *Goussia janae*. Fig. 22. An early macrogametocyte containing a large endoplasmic reticulum (ER), lipid inclusions (LI), dense granules (DG), and amylopectin granules (AG). × 11 000. Fig. 23. Projections of the enterocyte and PV membranes covering a maturing macrogametocyte. Large round granules with nonhomogeneous contents are present in the cytoplasm. × 20 500. Fig. 24. Multiple fusions with the microvilli at the tips of the projections (asterisks) leading to the formation of a spider-like macrogametocyte. × 22 400. Fig. 25. An oval mature macrogametocyte. Note that there are fewer lipid inclusions (LI) and more amylopectin granules (AG) than in the younger stages. The dense granules (DG) are almost centrally located, while multiple arrays of endoplasmic reticulum are arranged peripherally. ×7500. Fig. 26. Maturing macrogametocyte with a peculiar location in the host cells. Note that owing to its spider-like projections (asterisks), it is intracellular and extracytoplasmic with respect to three neighbouring enterocytes (HC1, HC2, HC3). PV, parasitophorous vacuole contents. ×6200.

FIGS. 27–31. Transmission electron micrographs showing microgametogenesis in *Goussia janae*. Fig. 27. Early microgametocyte with nuclei irregularly scattered in its cytoplasm. ×6000. Fig. 28. More advanced microgametocyte with peripherally located nuclei and the first emerging microgametes (arrows). ×7600. Fig. 29. Homogeneously dense part of the nucleus (DN) detached into the parasitophorous vacuole (PV) leaving remnants of the nucleus (RN) in the residual cytoplasm. The elongate mitochondrion (Mt) and flagella (Fl) became attached to a newly formed microgamete. × 26 000. Fig. 30. Large, mature microgametocyte. Numerous flagellated microgametes are accompanied by residual cytoplasm (RC). ×8300. Fig. 31. Slightly curved prominent perforatorium (arrowhead) of a mature microgamete. × 40 000.

veil formed by two loose membranes accompanying the suture were visible.

In sporulated oocysts the oocyst wall was composed of two layers, the outer of which was electron-transparent (about 9 nm thick) and the inner one electron-dense (about 27 nm thick) (Fig. 39).

The mature sporozoites in our material were poorly preserved; however, at least three pairs of long, homogeneously dense rhoptries and numerous thin micronemes could be discerned in the apical part of some sporozoites (Fig. 41).

Dense precipitates

Transmission electron microscopy

Dense precipitates were found after fixation with either osmium tetroxide or glutaraldehyde, followed by embedding in Epon–Araldite, and also in the portion of the studied material that was fixed with paraformaldehyde and embedded in LR White resin. Thin sections revealed the presence of precipitates after staining with both uranyl acetate and lead citrate and with Sato's lead stain. They were also present after en bloc staining with uranyl acetate or treating the sections with either 0.5 HCl or 1% EDTA.

The dense inclusions were situated in all compartments of the parasitic cell (cytoplasm, Golgi apparatus, mitochondria, nucleus, cytoplasmic vacuole) and in the PV contents. The inclusions were most frequently present in the cytoplasm and PV contents. However, the frequency of inclusions declined with the parasite's development, so whilst they were found in almost all merogonial stages, they were rarely found in the

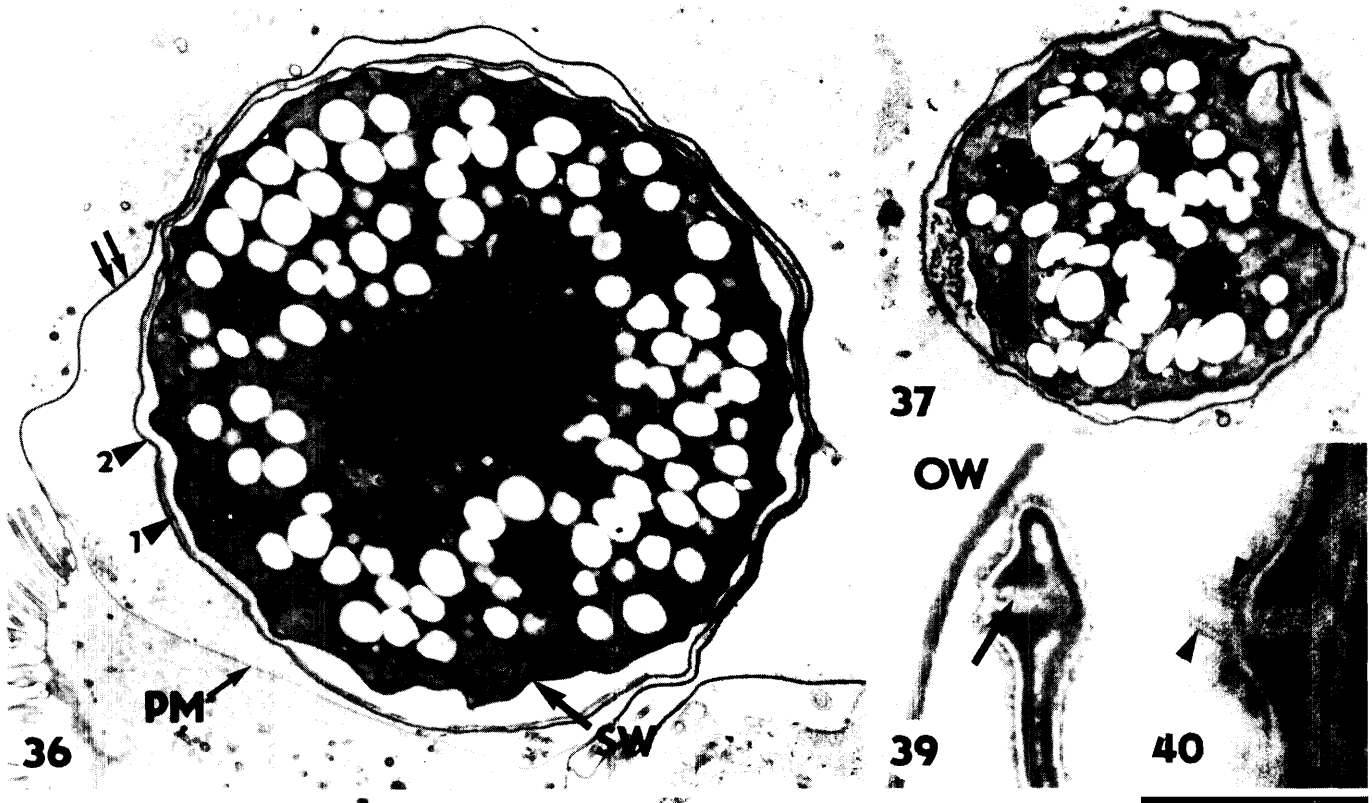

sporogonial stages. The precipitates were not found outside the PV membrane, i.e., in the enterocytes, goblet-cell cytoplasm, or gut lumen. They were always homogeneously electron-dense, nearly spherical in shape, and 20–80 nm in diameter.

X-ray microanalysis

For qualitative (semiquantitative in the sense of higher or lower X-ray intensity) measurements, only precipitates located in the cytoplasmic and parasitophorous vacuoles were selected, to reduce interference from the surrounding material (Figs. 49–51). Spectra from the enterocyte cytoplasm (Figs. 52, 53), parasite cytoplasm (Figs. 54, 55) and background resin (Figs. 56, 57) were used as controls.

Microprobe analysis of precipitates from unstained osmium-tetroxide-fixed samples indicated the presence of the following elements (element lines; the energy of the line (in keV) is given in parentheses (Goldstein et al. 1981)): OsM_α (1.910), PK_α (2.014), ClK_α (2.622), KK_α (3.314), CaK_α (3.692), NiK_α (7.478), CuK_α (8.048), ZnK_α (8.639), CuK_β (8.904), OsL_α (8.910). The large peaks of Cu, Ni, and Cl arised from the Cu or Ni grids and from the Epon–Araldite resin, respectively (compare with controls, Figs. 54 and 56). The peak KK_α was low, and in some measurements it was not at all well defined. The OsM_α line partially overlaps the PK_α line and similarly, the OsL_α line overlaps the CuK_β line (8.904 keV). To distinguish Os from P, and thus to reveal if Os is present in precipitates from osmicated samples, it was necessary to use the Ni grids as a support for some thin sections because the OsL_α line does not interfere with any Ni line (NiK_α, −7.478 keV, NiK_β, −8.264 keV) (Fig. 50). The low peak of the OsL_α line clearly indicated that Os is a minor component and P is a major component of the interaction volume containing the inclusions in an osmicated sample. The CaK_α peak was most prominent when the spectrum of inclusions was compared with the controls (Figs. 52, 54, 56).

Analysis of precipitates from paraformaldehyde-fixed (e.g., non-osmicated) and LR White-embedded samples also revealed high concentrations of Ca and P (Fig. 51) compared with the relevant controls (Figs. 53, 55, 57). The peak of the ZnK_α line was visible in precipitates from both osmicated and non-osmicated samples, and was absent in Epon–Araldite and LR White backgrounds. In the samples analyzed on Cu grids, the ZnK_α peak partly overlapped that of CuK_β (Figs. 49, 51); however, it was clearly defined on the spectra from Ni grids (Fig. 50). The measurements of Epon–Araldite and LR White resin backgrounds revealed the presence of Cl in the former resin and its absence in the latter one (Figs. 56, 57).

Discussion

In the last decade the genus *Goussia* (Labbé, 1896) has been considerably expanded by fish coccidia that were either newly described (Alvarez-Pellitero and Gonzales-Lanza 1985; Li and Desser 1985; Molnár and Rhode 1988) or transferred from the genus *Eimeria* after confirmation of a suture in their sporocyst wall (Dyková and Lom 1981).

Although the life-cycle stages of most members of the genus *Goussia* are localized intracytoplasmically (i.e., in the parasitophorous vacuole in the host-cell cytoplasm), the locations of at least seven species are quite different. Six of them, including *Goussia janae*, have been described from the gut epithelium (see Lukeš 1992*a*) and *G. spraguei* (Morrison and Poynton 1989) has been described from the kidney epithelium.

All developmental stages of the aforementioned species were localized in the microvillous region of the host cells. On the basis of light microscopic studies, this location was considered to be epicellular or epiepithelial (Landsberg and Paperna 1987; Molnár 1986, 1989; Molnár and Rhode 1988; Lukeš and Dyková 1990). However, recent ultrastructural studies have made it clear that these species are localized intracellularly and extracytoplasicmally (Morrison and Poynton 1989; Jastrzebski and Komorowski 1990; Lukeš 1992*a*).

The merogonial, gamogonial, and early sporogonial stages of *G. janae* were separated from the gut lumen by two closely apposed host-cell-derived membranes (the enterocyte and PV membranes). On the host–parasite interface of *G. janae*, the PV membrane was simply stretched round the coccidium, forming no projections or undulations.

Infections commenced with the invasion of the enterocyte by a motile zoite. In Fig. 2 its apical part is shown coming into contact with the glycocalyx, which is visible in fish enterocytes as a fuzzy coating on the tips of the microvilli (Strohband and Debets 1978; Albertini-Berhaut 1988). This contact might represent the first step in host-cell recognition prior to invasion, as described in other apicomplexans (Braun Breton and

FIGS. 32–42. Transmission and scanning electron micrographs of sporogonial stages and mature oocysts of *Goussia janae*. Figs. 32–36. Formation of oocyst and sporocyst walls during endogenous sporulation. Pe, pellicle; arrowheads 1 and 2, two layers constituting future oocyst wall; small arrows, enterocyte and parasitophorous vacuole membranes; SW, sporocyst wall; PM, parasitophorous vacuole membrane. Fig. 32. Single layer (arrowhead 2) detached from the sporont cytoplasm, while another layer (arrowhead 1) remains joined to the trilaminar pellicle. Note the multiple arrays of endoplasmic reticulum (ER). The asterisk indicates a microporus. × 47 000. Fig. 33. After both layers detach from the sporont cytoplasm they become closely apposed to each other. The sporocyst wall has not so far formed. × 47 000. Fig. 34. The luminal part of a mature sporont shortly before it detaches into the gut lumen. The foundations of the oocyst and sporocyst walls have already formed. × 105 000. Fig. 35. The host–parasite interface of the stage shown in Fig. 34. Note that only the parasitophorous vacuole membrane (PM) separates the parasite from the host-cell cytoplasm (HC). × 105 000. Fig. 36. A mature sporont with the foundations of the oocyst and sporocyst walls. Its cytoplasm is filled with amylopectin granules. The internal layer of the oocyst wall (arrowhead 1) has ruptured into several fragments as a result of the fixation process. ×9600. Fig. 37. A mature sporont within casts in the gut lumen. The sporont cytoplasm is covered by the completely formed oocyst wall and the foundations of the sporocyst wall. ×8100. Fig. 38. Exogenously sporulated oocyst. In this section two sporocysts, each containing two immature sporozoites, are visible. Note the large crystalloid bodies (arrows) within the sporozoite cytoplasm. Owing to shrinkage of the cytoplasm, the oocyst and sporocyst walls have formed artefactual projections. ×9300. Fig. 39. The oocyst wall (OW) and sporocyst wall bearing the suture of a sporulated oocyst. Shrinkage of the sporocyst cytoplasm has resulted in the formation of an artefactual projection of the sporocyst wall, the tip of which is shown here. A thin interposing strip (arrow) inserted in the suture is visible. × 120 000. Fig. 40. Suture in the sporocyst wall of a sporulated oocyst. Note the tiny membranaceous veil (arrows) along the suture. × 185 000. Fig. 41. Apical portion of a mature sporozoite within a sporocyst. Rh, rhoptries; Mi, micronemes; the arrow indicates the suture. Fig. 42. Two mature elongate sporozoites within the transparent sporocyst wall. A longitudinal suture is visible in the sporocyst wall (arrows). ×4200.

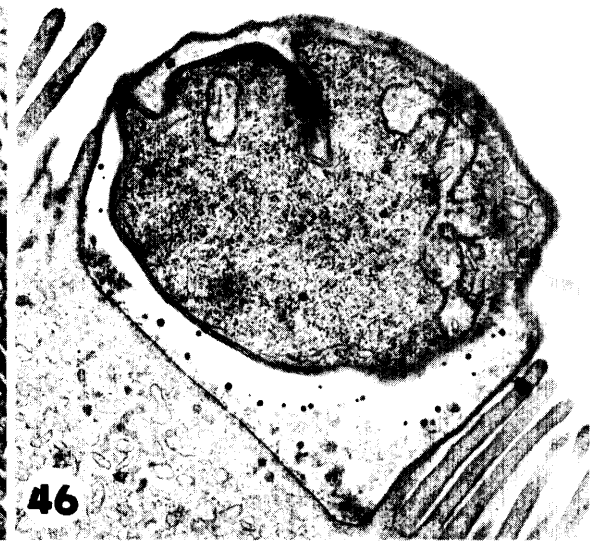

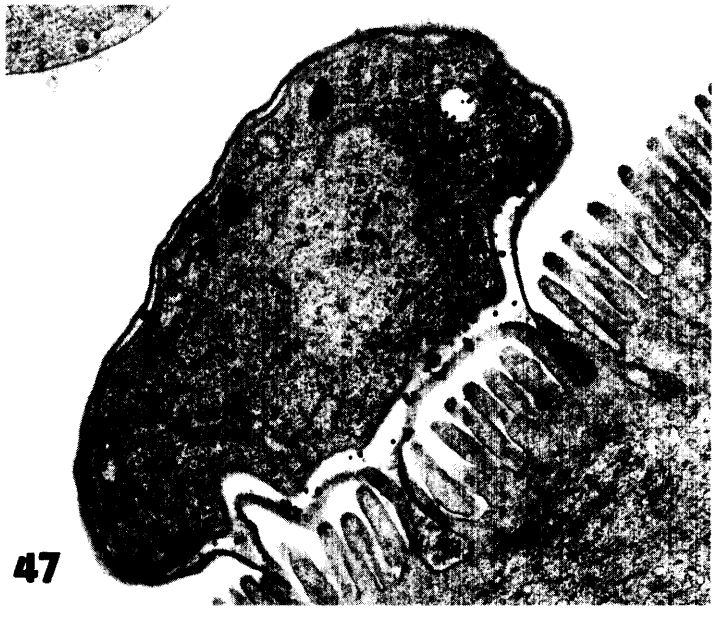

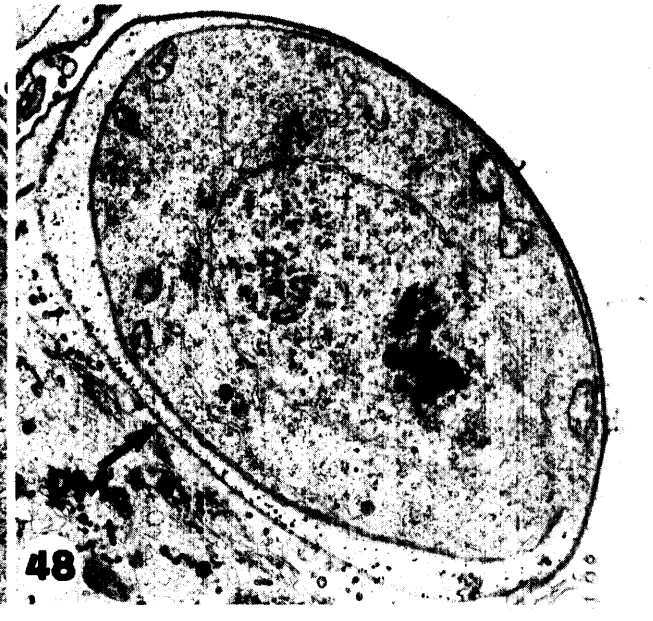

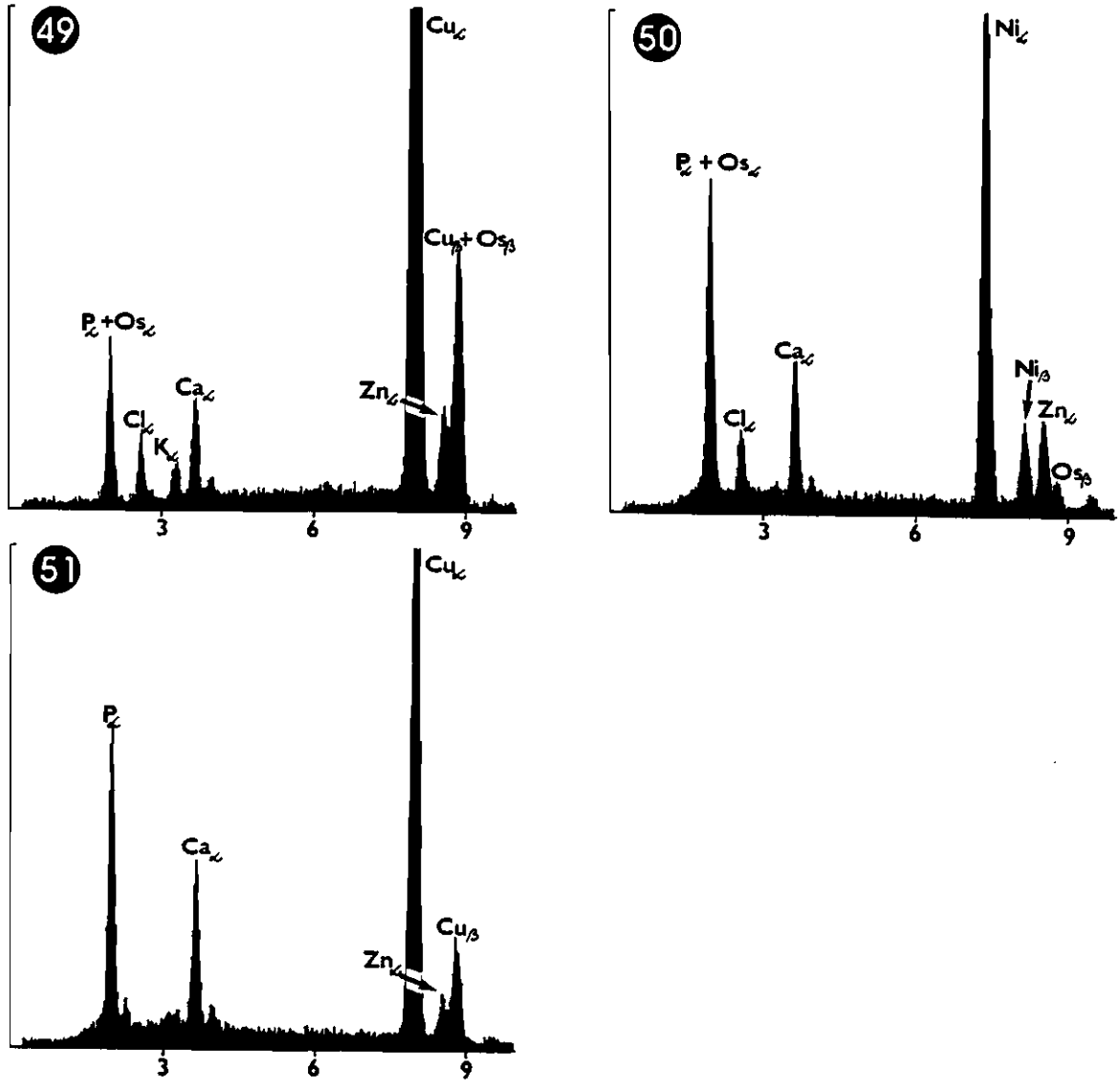

FIGS. 49–51. X-ray microanalysis spectra of precipitates. Fig. 49. Osmicated sample on the Cu grid. Fig. 50. Osmicated sample on the Ni grid. Fig. 51. Non-osmicated sample on the Cu grid. The *x*-axis shows X-ray energy (keV); the *y*-axis shows the relative number of counts.

Pereira da Silva 1989). Although we could not perceive the moment of the host-cell entry, we assume that the mechanism is similar to that described for *Cryptosporidium* sp. in cultures of Madin–Darby canine kidney cells (Lumb et al. 1988) and an EC coccidium *Eimeria* sp. from the intestinal epithelium of a gecko (Paperna 1989).

After the intracellular position of the zoite was established, further development led to the formation of either a monopodial or a spider-like meront. The process during which both types of location in the host cell are formed has recently been described in detail for *Goussia pannonica* (Lukeš 1992*a*), and seems to be almost the same in *G. janae*, consisting also of multiple fusions of the enterocyte membrane stretched round the parasite to microvilli of the same or neighbouring enterocytes. The lateral fusions lead to the formation of a monopodial stage with a single zone of attachment which is common to all EC species described hitherto. The fusions with separate microvilli produce a spider-like stage localized above the microvillous zone. Through multiple projections it is connected either with a single enterocyte or, rarely, with more host cells. It is thus intracellular and EC for all of them (Figs. 13, 26). Until now the spider-like stages have been described in *Acroeimeria lineri* from the gecko (Paperna and Landsberg 1989), *Haemogregarina balli* from a leech (Siddall and Desser

FIGS. 43–48. Dense precipitates in the merogonial stages of *Goussia janae* (Figs. 43, 44, and 48) and *G. pannonica* (Figs. 45–47). Fig. 43. Spider-like meront containing precipitates that are predominantly located in the contents of the cytoplasmic vacuoles. × 20 000. Fig. 44. Spider-like meront with numerous small precipitates in its cytoplasm only. × 40 000. Fig. 45. A rare occurrence of large precipitates in the nucleus (Nu), mitochondrion (Mt), and Golgi apparatus (GA). × 28 000. Fig. 46. Early monopodial meront with precipitates restricted to the parasitophorous vacuole contents. × 20 700. Fig. 47. Early spider-like meront containing multiple precipitates in the cytoplasmic and parasitophorous vacuoles contents. × 17 600. Fig. 48. Multiple precipitates distributed in the parasitophorous vacuole of a large mature meront. Note their absence outside the parasitophorous vacuole membrane (PM). × 13 000.

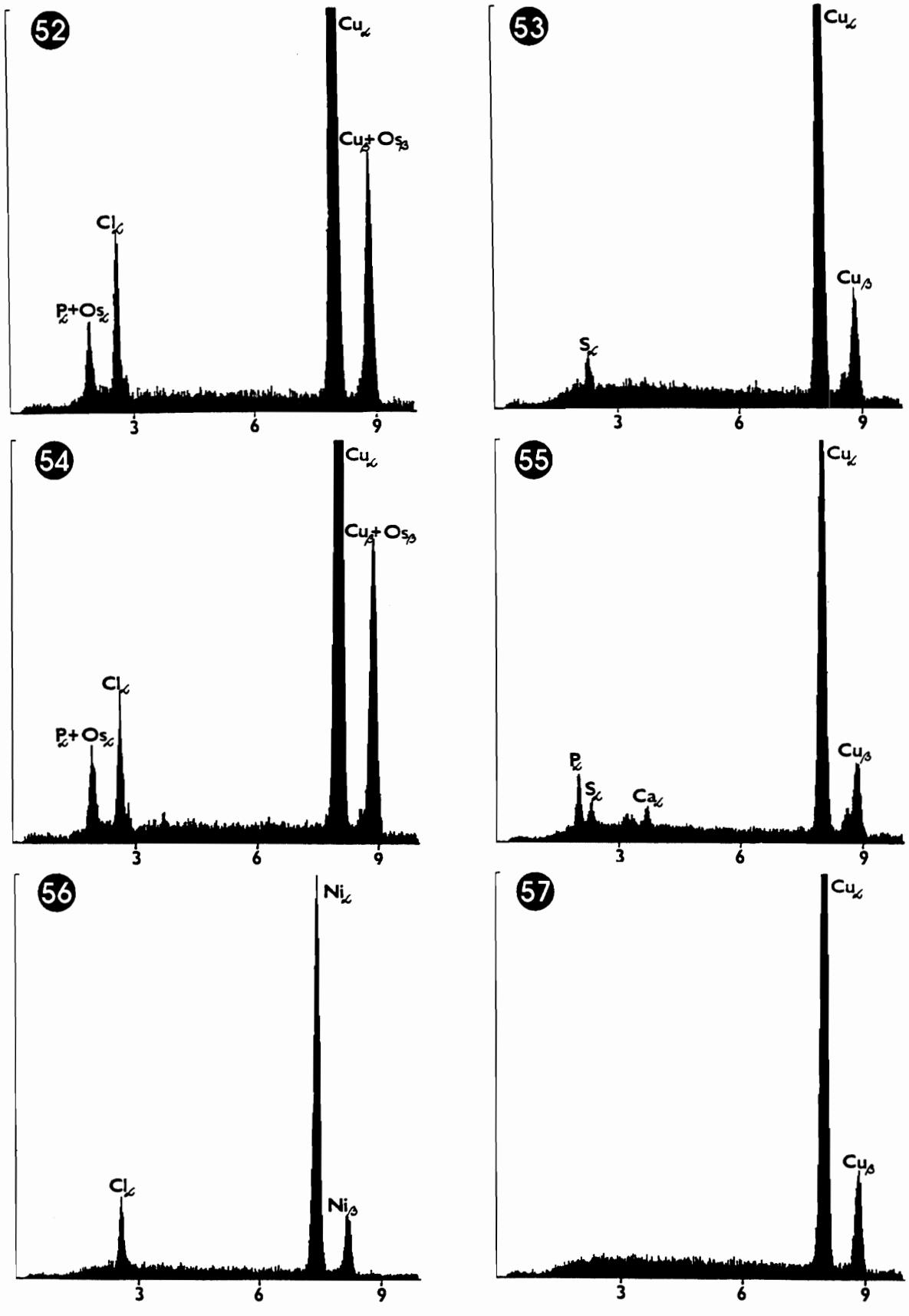

FIGS. 52 and 53. X-ray microanalysis spectra of enterocyte cytoplasm. Fig. 52. Osmicated sample on the Cu grid. Fig. 53. Non-osmicated sample on the Cu grid. FIGS. 54–55. X-ray microanalysis spectra of parasite cytoplasm. Fig. 54. Osmicated sample on the Cu grid. Fig. 55. Non-osmicated sample on the Cu grid. FIGS. 56 and 57. X-ray microanalysis spectra of the resin backgrounds. Fig. 56. Epon–Araldite resin on the Ni grid. Fig. 57. LR White resin on the Cu grid. The *x*-axis shows X-ray energy (keV); the *y*-axis shows the relative number of counts.

1990), *G. pannonica* and *G. janae* from bream and from chub and dace, respectively (Lukeš 1992*a*; this paper).

The substantial growth of the parasite in the microvillous region from small meronts (about 3.5 μm in diameter; Figs. 4, 5) into large oval sporonts (about 13 × 10 μm; Fig. 36) leads inevitably to the gradual stretching of both covering membranes. Although we can only speculate on the biological significance of the fusions of the enterocyte membrane covering the coccidium with neighbouring microvilli, it seems probable that they enable the membrane to continuously enlarge. The growth and functions of the PV membrane could be directly affected by the parasite through processes similar to those described in other coccidia (Bannister and Dluzewski 1990; Dubremetz 1990). This concept is supported by the behaviour of the PV membrane during the establishment of a new attachment area of a spider-like stage. After the enterocyte membrane covering the parasite fused to a microvillus (or microvilli), the PV membrane passed through the lumen of a newly fused microvillus until it reached the cytoplasm of the host cell. Thus, a new host–parasite interface became established.

In tissues heavily infected with the EC stages of *G. janae*, intracellular (IC) stages have sometimes been observed also (Lukeš and Dyková 1990). Although members of the genus *Epieimeria* have an EC merogony and gamogony and IC sporogony (Dyková and Lom 1981; Lacey and Williams 1983; Daoudi et al. 1987), it is now obvious that this is not the case in *G. janae*. In the early spring, when the infections culminated, the dace and chub concurrently harboured EC and IC stages, although these belonged to different species, as was unambiguously expressed by the discharge of morphologically different oocysts (Lukeš 1992*b*).

The data on the merogonial sequence of EC coccidia are insufficient, with the exception of *G. pannonica* and *Eimeria vanasi*, where ectomerogony, endodyogony, and endopolygony have been documented (Landsberg and Paperna 1987; Paperna 1991; Lukeš 1992*a*). At least two types of meront have been described from the EC species *Epieimeria anguillae* and *Goussia girellae*, though the type of merogony was not specified (Molnár and Baska 1986; Kent et al. 1988). The combination of merogonial divisions described herein (i.e., ecto- and endo-merogony) has been described only for an IC species of fish coccidium, *Goussia iroquina* (see Paterson and Desser 1981).

The microgametogenesis that resulted in the formation of biflagellate microgametes at the periphery of the microgamont was similar to the same sequence in other EC species (Molnár and Baska 1986; Morrison and Poynton 1989; Jastrzebski and Komorowski 1990). During macrogametogenesis, the cytoplasm became filled with lipid and, especially, with amylopectin granules. The round, nonhomogeneously dense granules present from the emergence of the early macrogamonts to the emergence of the sporonts were comparable to the wall-forming bodies of type II of Chobotar and Scholtysek (1982). However, the present ultrastructural study supports our opinion that if granules similar to wall-forming bodies are present in fish coccidia, they cannot have participated in the formation of the oocyst envelope in the way that has been described for coccidia from warm-blooded vertebrates (Mehlhorn 1988).

Multiple arrays of endoplasmic reticulum subtending the pellicle of early sporonts indicated the crucial role of this organelle in the formation of two layers that detached consecutively from the sporont cytoplasm. The significance of these layers to the future oocyst wall was made clear after the sporocyst wall formed beneath them. The rupture of both host-cell-derived membranes finished the IC and EC phases of the life cycle, hence sporulation continued exogenously in the surrounding water. Although several authors have described the participation of a host cell in oocyst-wall formation in fish coccidia (Hawkins et al. 1983; Desser and Li 1984; Morrison and Hawkins 1984; Morrison and Poynton 1989; Jastrzebski and Komorowski 1990), we could not find any support for this unusual mechanism in our material. The oocyst wall of *G. janae* was produced entirely by the sporont itself, and this is in accordance with recent papers dealing with sporulation of fish coccidia (Baska and Molnár 1989; Davies 1990; Lom et al. 1991; Lukeš 1992*a*).

The disruption of the oocyst and sporocyst walls in the homogenizer enabled us to study sporulated oocysts, the ultrastructure of which is usually poorly preserved, owing to the low permeability of the oocyst walls to fixatives (Beesley and Latter 1982). Based on the presence of the suture in the sporocyst wall, accompanied by a tiny membranaceous veil, *G. janae* belongs to the subgenus *Plagula* (Overstreet et al. 1984). Among the ultrastructural features of the sporozoites, a large crystalloid body should be noted. Among terrestrial coccidia, this body is typical of members of the genus *Isospora* (Chobotar and Scholtysek 1982), but among fish coccidia, it has been found in the sporozoites of species of both *Eimeria* (Desser and Li 1984; Morrison 1991) and *Goussia* (Paperna and Landsberg 1985; Morrison and Poynton 1989; Lukeš 1992*a*; this paper). Our initial conclusion that the fine, electron-dense precipitates represent contamination was disproved by their selective distribution in the thin sections. They only appeared in the parasite cytoplasm, cytoplasmic vacuoles, and more frequently in the PV contents. They have very rarely been observed in the parasite nucleus.

The artefactual deposits in fixed and embedded tissues described by several authors can be divided into two groups. The first type can be removed by treating thin sections with various chemicals (Ellis and Anthony 1980; Mollenhauer 1987). The other, more frequent type of artefactual deposit appeared after various combinations of phosphate or Millonig buffers, Karnovsky, glutaraldehyde and (or) osmium tetroxide fixation, and uranyl acetate staining were used (Kuthy and Csapó 1976; Hendriks and Eestermans 1982; Louw et al. 1990). We were unsuccessful in removing the precipitates, either by various combinations of fixation, embedding, and staining procedures, or by additional treatment of the thin sections. Therefore, we consider the precipitates in our material to have a different origin from the aforementioned deposits, although their morphological resemblance was close.

Investigation of the precipitates in question by energy-dispersive semiquantitative X-ray microanalysis produced interesting results. The presence of high peaks of Os, Cl, Cu, and Ni was due to the use of osmium tetroxide fixative, Epon–Araldite resin, and Cu and Ni grids, respectively. The use of Cu and Ni grids as supports for the thin sections of osmicated samples indicated clearly that the Os peak in dense precipitates is very low and, moreover, can be due to a signal from the surrounding material. This measurement finally differentiated these granules from morphologically similar ones, in which a high concentration of Os has been detected (Hendrick and Eestermans 1982). The presence of Zn could not be satisfactorily explained. In our opinion, the only source of this biologically unusual element could have been the highly

polluted water of the Černovický Potok Brook, where the infected fish were caught.

The elevated Ca and P levels in the dense precipitates may indicate the presence of calcium hydroxyapatite, $(Ca_3(PO_4)_2)_3\ Ca(OH)_2$, originally described in inclusions from rat liver michondria by Greenawalt et al. (1964). Since then, precipitates containing this compound have been demonstrated in the lumen of mitochondria from various cells (e.g., Pedersen et al. 1978; Tzagoloff 1982; Ude and Koch 1982). Large electron-dense inclusions with the same contents have been described from hydrogenosomes isolated from cells of the protozoon *Trichomonas vaginalis* (Chapman et al. 1985). Both mitochondria and hydrogenosomes are involved in calcium uptake within the cell (Tzagoloff 1982; Chapman et al. 1985). The calcium hydroxyapatite granules mirror unusually high Ca and P levels in the parasitophorous vacuole of developmental stages of *G. janae* (Figs. 8, 12, 22, 43, 44, 48) and *G. pannonica* (Figs. 45–47). The same precipitates also occurred in other extracytoplasicmally located coccidia studied by us (Lukeš 1992*a*; J. Lukeš, unpublished data), and their presence can be discerned in micrographs of other species (Ostrovska and Paperna 1987; Paperna 1989; Jastrzebski and Komorowski 1990). The occurrence of these precipitates may reflect some metabolic specificity involving Ca in EC coccidia.

Acknowledgements

We thank Drs. Jiří Lom and Iva Dyková, Institute of Parasitology, Czech Academy of Sciences, for continuous support and for reading the manuscript. We also thank Dr. František Weyda, Institute of Entomology, Czech Academy of Sciences, Prof. Jaroslav Kulda, Department of Parasitology, Charles University, and Jana Nebesářová, Electron Microscopy Unit, Czech Academy of Sciences, for their helpful comments and suggestions. The help of Tomáš Kepr, Institute of Parasitology, in collecting some of the material is acknowledged.

Albertini-Berhaut, J. 1988. L'intestin chez les Mugilidae (Poissons Téléostéens) à différentes étapes de leur croissance. II. Aspects ultrastructuraux et cytophysiologiques. J. Appl. Ichthyol. **4**: 65–78.

Alvarez-Pellitero, M. P., and Gonzáles-Lanza, M. C. 1985. *Goussia polylepidis* n.sp. (Apicomplexa: Sporozoea: Coccidia) from *Chondrostoma polylepis* (Pisces: Cyprinidae) of the Duero Basin (NW Spain). J. Protozool. **32**: 570–571.

Bannister, L. H., and Dluzewski, A. R. 1990. The ultrastructure of red cell invasion in malaria infection: a review. Blood Cells, **16**: 257–292.

Baska, F., and Molnár, K. 1989. Ultrastructural observations on different developmental stages of *Goussia sinensis* (Chen, 1955), a parasite of the silver carp (*Hypophthalmichthys molitris* Vallenciennes, 1844). Acta Vet. Hung. **37**: 81–87.

Beesley, B., and Latter, V. S. 1982. The sporulation of *Eimeria tenella* as revealed by a novel preparative method. Z. Parasitenkd. **67**: 255–260.

Braun Breton, C., and Pereira da Silva, L. H. 1989. Modulation de l'activité biologique des protéines de surface chez les protozoaires hémoparasites. Méd. Sciences, **5**: 736–743.

Chapman, A., Hann, A. C., Linstead, D., and Lloyd, D. 1985. Energy-dispersive X-ray microanalysis of membrane-associated inclusions in hydrogenosomes isolated from *Trichomonas vaginalis*. J. Gen. Microbiol. **131**: 2933–2939.

Chobotar, B., and Scholtysek, E. 1982. Ultrastructure. *In* The biology of the coccidia. *Edited by* P. L. Long. University Park Press, London, pp. 101–167.

Current, W. L., and Reese, N. C. 1986. A comparison of endogenous development of three isolates of *Cryptosporidium* in suckling mice. J. Protozool. **33**: 98–108.

Daoudi, F., Radujkovič, B., Marquès, A., and Bouix, G. 1987. Nouvelles espèces de Coccidies (Apicomplexa, Eimeriidae) des genres *Eimeria* Schneider, 1875, et *Epieimeria* Dyková et Lom, 1981, parasites de poissons marins de la baie de Kotor (Yougoslavie). Bull. Mus. Nat. Hist. Nat. Paris, **9**: 321–332.

Davies, A. J. 1990. Ultrastructural studies on the endogeneous stages of *Eimeria variabilis* (Thélohan, 1893) Reichenow, 1921, from *Cottus* (*Taurulus*) *bubalis* Euphrasen (Teleostei: Cottidae). J. Fish Dis. **13**: 447–461.

Desser, S. S., and Li, L. 1984. Ultrastructural observations on the sexual stages and oocyst formation in *Eimeria laureleus* (Protozoa, Coccidia) of perch, *Perca flavescens*, from Lake Sasajewun, Ontario. Z. Parasitenkd. **70**: 153–164.

Dubremetz, J. F. 1990. Caractéristiques communes de l'invasion de la cellule-hote par les sporozoaires. Ann. Parasitol. Hum. Comp. **65**(Suppl. I): 23–25.

Dyková, I., and Lom, J. 1981. Fish coccidia: critical notes on life cycles, classification and pathogenicity. J. Fish Dis. **4**: 487–505.

Ellis, E. A., and Anthony, D. W. 1980. A method for removing precipitate from ultrathin sections resulting from glutaraldehyde-osmium tetroxide fixation. Stain Technol. **54**: 282–285.

Goldstein, J., Newbury, D. E., Echlin, P., Joy, D. C., Fiori, C., and Lifshin, E. 1981. Scanning electron microscopy and X-ray microanalysis. Plenum Press, New York and London. pp. 641–643.

Greenawalt, J. W., Rossi, C. S., and Lehninger, A. L. 1964. Effect of active accumulation of calcium and phosphate ions on the structure of rat liver mitochondria. J. Cell Biol. **23**: 21–37.

Hanaichi, T., Sato, T., Iwamoto, T., Malavashi-Yamamoto, J., Hoshino, M., and Mizuno, N. 1986. A stable lead by modification of Sato's method. J. Electron Microsc. **35**: 304–306.

Hawkins, W. E., Fournie, J. W., and Overstreet, R. M. 1983. Organization of sporulated oocysts of *Eimeria funduli* in the gulf killifish, *Fundulus grandis*. J. Parasitol. **69**: 496–503.

Hayat, M. A. 1975. Positive staining for electron microscopy. Van Nostrand Reinhold Company, New York. pp. 45–68.

Hendriks, H. R., and Eestermans, I. L. 1982. Electron dense granules and the role of buffers: artefacts from fixation with glutaraldehyde and osmium tetroxide. J. Microsc. **126**: 161–168.

Jastrzebski, M., and Komorowski, Z. 1990. Light and electron microscopic studies on *Goussia zarnowskii* (Jastrzebski, 1982)—an intestinal coccidium parasitizing the three-spined stickleback, *Gasterosteus aculeatus*. J. Fish Dis. **13**: 1–24.

Kent, A. P., and Kendall, M. D. 1988. The use of the acrylic resin LR White in the estimation of elemental sulphur by X-ray microanalysis. Proc. Microsc. Soc. **23**: 213 A.

Kent, M. L., Fournie, J. W., Snodgrass, R. E., and Elston, R. A. 1988. *Goussia girellae* n.sp. (Apicomplexa, Eimeriorina) in the opaleye, *Girella nigricans*. J. Protozool. **35**: 287–290.

Kuthy, E., and Csapo, Z. 1976. Peculiar artefacts after fixation with glutaraldehyde and osmium tetroxide. J. Microsc. **107**: 177–182.

Lacey, S. M., and Williams, I. C. 1983. *Epieimeria anguillae* (Léger and Hollande, 1922) Dyková and Lom 1981 (Apicomplexa, Eucoccidia) in the European eel, *Anguilla anguilla* (L.). J. Fish Biol. **23**: 605–609.

Landsberg, J. H., and Paperna, I. 1987. Intestinal infections by *Eimeria* (s.l.) *vanasi* n.sp. (Eimeriidae, Apicomplexa, Protozoa) in cichlid fish. Ann. Parasitol. Hum. Comp. **62**: 283–293.

Li, L., and Desser, S. S. 1985. The protozoan parasites of fish from two lakes in Algonquin Park, Ontario. Can. J. Zool. **63**: 1846–1858.

Lom, J., Steinhagen, D., Körting, W., and Dyková, I. 1991. Oocyst formation in the coccidian parasite *Goussia carpelli*. Dis. Aquat. Org. **10**: 203–209.

Louw, J., Williams, K., Harper, I. S., and Walfe-Coote, S. A. 1990. Electron dense artefactual deposits in tissue sections: the role of ethanol, uranyl acetate and phosphate buffer. Stain Technol. **65**: 243–250.

Lukeš, J. 1992*a*. Life cycle of *Goussia pannonica* (Molnár, 1989) (Apicomplexa, Eimeriorina), an extracytoplasmic coccidium from the white bream, *Blicca bjoerkna*. J. Protozool. **39**: 484–494.

Lukeš, J. 1992*b*. Concurrent infections of extra- and intracytoplasmic fish coccidia. Acta Soc. Zool. Bohemoslov. **56**: 76A.

Lukeš, J., and Dyková, I. 1990. *Goussia janae* n.sp. (Apicomplexa, Eimeriorina) in dace *Leuciscus leuciscus* and chub *L. cephalus*. Dis. Aquat. Org. **8**: 85–90.

Lumb, R., Smith, K., O'Donoghue, P. J., and Lanser, J. A. 1988. Ultrastructure of the attachment of *Cryptosporidium* sporozoites to tissue culture cells. Parasitol. Res. **74**: 531–536.

Mehlhorn, H. 1988. Morphology. *In* Parasitology in focus: facts and trends. *Edited by* H. Mehlhorn. Springer-Verlag, Stuttgart. pp. 161–188.

Mollenhauer, H. H. 1987. Contamination of thin sections: some observations on the cause and elimination of "embedding pepper." J. Electron Microsc. Tech. **5**: 59–63.

Molnár, K. 1986. Occurrence of two new *Goussia* species in the intestine of the sterlet (*Acipenser ruthenus*). Acta Vet. Hung. **34**: 169–174.

Molnár, K. 1989. Nodular and epicellular coccidiosis in the intestine of cyprinid fishes. Dis. Aquat. Org. **7**: 1–12.

Molnár, K., and Baska, F. 1986. Light and electron microscopic studies on *Epieimeria anguillae* (Léger and Hollande, 1922), a coccidium parasitizing the European eel, *Anguilla anguilla* L. J. Fish Dis. **9**: 99–110.

Molnár, K., and Rhode, K. 1988. New coccidians from freshwater fishes of Australia. J. Fish Dis. **11**: 161–169.

Morrison, C. M. 1991. Further observations on the sporogony of *Eimeria sardinae* in the testis of the herring *Clupea harrengus* L. Can. J. Zool. **69**: 1017–1024.

Morrison, C. M., and Hawkins, W. E. 1984. Coccidians in the liver and testis of the herring *Clupea harrengus* L. Can. J. Zool. **62**: 480–493.

Morrison, C. M., and Poynton, S. L. 1989. A new species of *Goussia* (Apicomplexa, Coccidia) in the kidney tubules of the cod, *Gadus morhua*. J. Fish Dis. **12**: 533–560.

Ostrovska, K., and Paperna, I. 1987. Ultrastructural studies on the merogony of *Schellackia* cf. *Agamae* (Lankesterellidae, Apicomplexa) from the starred lizard *Agama stellio*. Ann. Parasitol. Hum. Comp. **62**: 380–386.

Overstreet, R. M., Hawkins, W. E., and Fournie, J. W. 1984. The coccidian genus *Calyptospora* n.g. and the family Calyptosporidae n.fam. (Apicomplexa) with members infecting primarily fishes. J. Protozool. **31**: 332–339.

Paperna, I. 1989. Ultrastructure of *Eimeria* (s.l.) sp. infecting the microvillar zone of the intestinal epithelium of geckoes. Ann. Parasitol. Hum. Comp. **64**: 89–99.

Paperna, I. 1991. Fine structure of *Eimeria* (s.l.) *vanasi* merogony stages in the intestinal mucosa of cichlid fishes. Dis. Aquat. Org. **10**: 195–201.

Paperna, I., and Landsberg, J. H. 1985. Ultrastructure of oogony and sporogony in *Goussia cichlidarum*, Landsberg and Paperna, 1985, a coccidian parasite in the swimbladder of cichlid fish. Protistologica, **21**: 349–359.

Paperna, I., and Landsberg, J. H. 1989. Description and taxonomic discussion of eimerian coccidia from African and Levantine geckoes. S. Afr. J. Zool. **24**: 345–355.

Patterson, W. B., and Desser, S. S. 1981. An ultrastructural study of *Eimeria iroquina* Molnár and Fernando, 1974, in experimentally infected fathead minnow (*Pimephales promelas*, Cyprinidae). 3. Merogony. J. Protozool. **28**: 302–308.

Pedersen, P. L., Greenawalt, J. W., Reynafarje, B., Hullihen, J., Decker, G. L., Soper, J. W., and Bustamente, E. 1978. Preparation and characterization of mitochondria and submitochondrial particles of rat liver and liver-derived tissues. Methods Cell Biol. **20**: 411–481.

Roth, J., and Heitz, P. U. 1989. Immunolabeling with the protein A-gold technique: an overview. Ultrastruct. Pathol. **13**: 467–484.

Siddall, M. E., and Desser, S. S. 1990. Gametogenesis and sporogonic development of *Haemogregarina balli* (Apicomplexa: Adeleida: Haemogregarinidae) in the leech *Placobdella ornata*. J. Protozool. **37**: 511–520.

Strohband, H. W. J., and Debets, F. M. H. 1978. The ultrastructure and renewal of the intestinal epithelium of the juvenile grasscarp, *Ctenopharyngodon idella* (Val.). Cell Tissue Res. **187**: 181–200.

Tzagoloff, A. 1982. Mitochondria. Plenum Press, New York and London. pp. 15–37.

Ude, J., and Koch, M. 1982. Die Zelle: Atlas der Ultrastruktur. VEB Gustav Fischer Verlag, Jena. pp. 70–88.

Venable, J. H., and Coggeshall, R. 1965. A simplified lead citrate stain for use in microscopy. J. Cell Biol. **5**: 163–193.

This article has been cited by:

1. De-Hua Lai, Esteban J. Bontempi, Julius Lukeš. 2012. Trypanosoma brucei solanesyl-diphosphate synthase localizes to the mitochondrion. *Molecular and Biochemical Parasitology* **183**:2, 189-192. [CrossRef]
2. De-Hua Lai, Esteban J. Bontempi, Julius Lukeš. 2012. Trypanosoma brucei solanesyl-diphosphate synthase localizes to the mitochondrion. *Molecular and Biochemical Parasitology* . [CrossRef]
3. De-Hua Lai, Esteban J. Bontempi, Julius Lukeš. 2012. Trypanosoma brucei solanesyl-diphosphate synthase localizes to the mitochondrion. *Molecular and Biochemical Parasitology* . [CrossRef]
4. S. Gibson-Kueh, N.T.N. Thuy, A. Elliot, J.B. Jones, P.K. Nicholls, R.C.A. Thompson. 2011. An intestinal Eimeria infection in juvenile Asian seabass (Lates calcarifer) cultured in Vietnam – A first report. *Veterinary Parasitology* . [CrossRef]